# Electro-optic narrowband multi-wavelength filter in aperiodically poled lithium niobate

**C. H. Lin,[1] Y. H. Chen,[1*] S. W. Lin,[1] C. L. Chang,[1] Y. C. Huang,[2] and J. Y. Chang[1]**

[1]*Department of Optics and Photonics, National Central University, Jhongli 320, Taiwan*
[2]*Institute of Photonics Technologies, National Tsing-Hua University, Hsinchu 300, Taiwan*
**Corresponding author: yhchen@dop.ncu.edu.tw*

**Abstract:** We report on an iterative design scheme for and the first experimental demonstration of active narrowband multi-wavelength filters based on aperiodically poled lithium niobate crystals. A simultaneous transmission of 8 wavelengths, each with a ~0.45-nm linewidth and nearly 100% peak transmittance, was achieved in such a device. The transmission spectrum of this device can be tuned by temperature at a rate of ~0.65 nm/°C.



**OCIS codes:** (230.2090) Electro-optical devices; (120.2440) Filters; (230.5440) Polarization-sensitive devices.

## References and links

1. R. R. Willey, "Achieving narrow bandpass filters which meet the requirements for DWDM," Thin Solid Films **398-399**, 1-9 (2001).
2. J. W. Evans, "Solc birefringent filter," J. Opt. Soc. Am. **48**, 142-145 (1958).
3. R. C. Alferness, "Efficient waveguide electro-optic TE↔TM mode converter/wavelength filter," Appl. Phys. Lett. **36**, 513-515 (1980).
4. R. C. Alferness and L. L. Buhl, "Electro-optic waveguide TE↔TM mode converter with low drive voltage," Opt. Lett. **5**, 473-475 (1980).
5. X. Chen, J. Shi, Y. Chen, Y. Zhu, Y. Xia, and Y. Chen, "Electro-optic Solc-type wavelength filter in periodically poled lithium niobate," Opt. Lett. **28**, 2115-2117 (2003).
6. Y. H. Chen and Y. C. Huang, "Actively Q-switched Nd:$YVO_4$ Laser Using an Electro-optic PPLN Crystal as a Laser Q-switch," Opt. Lett. **28**, 1460-1462 (2003).
7. J. Wu, T. Kondo and R. Ito, "Optimal Design for Broadband Quasi-Phase-Matched Second-Harmonic Generation Using Simulated Annealing," J. Lightwave Technol. **13**, 456-460 (1995).
8. S. Kirkpatrick, C. D. Gelatt, and M. P. Vecchi, "Optimization by simulated annealing," Science **220**, 671-680 (1983).
9. Y. W. Lee, F. C. Fan, Y. C. Huang, B. Y. Gu, B. Z. Dong, M. H. Chou, "Nonlinear multiwavelength conversion based on an aperiodic optical superlattice in lithium niobate," Opt. Lett. **27**, 2191-2193 (2002).
10. A. Yariv, "Coupled-mode theory for guided-wave optics," IEEE J. Quantum Electron. **QE-9**, 919-933 (1973).
11. B. Y. Gu, Y. Zhang, and B. Z. Dong, "Investigations of harmonic generations in aperiodic optical superlattices," J. Appl. Phys. **87**, 7629-7637 (2000).
12. X. Gu, X. Chen , Y. Chen, X. Zeng, Y. Xia, and Y. Chen, "Narrowband multiple wavelengths filter in aperiodic optical superlattice," Opt. Comm. **237**, 53-58 (2004).
13. L. E. Myers, R. C. Eckardt, M. M. Fejer, R. L. Byer, W. R. Bosenberg, and J. W. Pierce, "Quasi-phase-matched optical parametric oscillators in bulk periodically poled $LiNbO_3$," J. Opt. Soc. Am. B **12,** 2102-2116 (1995).
14. C. Y. Huang, C. H. Lin, Y. H. Chen, and Y. C. Huang, "Electro-optic Ti:PPLN waveguide as efficient optical wavelength filter and polarization mode converter," Opt. Exp. **15**, 2548-2554 (2007).
15. M. M. Fejer, G. A. Magel, D. H. Jundt, and R. L. Byer, "Quasi-phase-matched second harmonic generation: tuning and tolerances," IEEE J. Quantum Electron. **23**, 2631-2654 (1992).

## 1. Introduction

Optical filters are indispensable elements in many optical systems for the processing of the spectral content of optical signals. Narrowband optical filters are particularly useful in the areas of optical signal processing and communications. Among the optical filter technologies,

#81954 - $15.00 USD Received 9 Apr 2007; revised 11 Jul 2007; accepted 17 Jul 2007; published 20 Jul 2007

multilayer optical thin-film coating [1] could be the most popular one. However, thin-film filters operate passively with fixed spectral characteristics. Evidently, an active and tunable optical filter would be very useful in applications requiring spectral adjustment. Šolc filters [2] are a kind of narrowband birefringence filter whose spectral transmission characteristics can be tuned by using the electro-optic (EO) effect or by varying the crystal angle to change the phase-retardation-matching condition in the filter. A conventional Šolc-type filter built in a single-domain birefringence crystal has to adopt a periodic electrode configuration to modulate the sign of the relevant EO coefficient so as to convert the polarization modes of the waves in it [3, 4]. Since the sign of the EO coefficient in a periodically pole crystal is periodically changed due to the periodic reversal of the crystal domain, a Šolc-type filter built into such a crystal can have a simpler electrode configuration, permitting the use of the full device length. The demonstration of Šolc-type filters in periodically poled lithium niobate (PPLN) crystals was recently reported with emphasis on *single-wavelength* spectral tuning [5] and power modulation [6].

Unlike the uniform grating structure commonly adopted by a PPLN crystal, an aperiodic grating can be implemented into a lithium niobate crystal to provide more than one grating vector from the spatially modulated domain lattice. The multiple grating vectors can be designed to simultaneously compensate for several wave-vector mismatches that arise from multiple wave-energy coupling processes in an optical medium. Such a scheme has been adopted by the so-called quasi-phase-matched (QPM) nonlinear wavelength conversion. For example, the concept of using an aperiodic grating structure has been applied to the design of a broadband QPM second-harmonic generator with the assistance of the simulated-annealing (SA) algorithm [7, 8]. More recently, aperiodically poled lithium niobate (APLN) crystals were also used for demonstrating equal-gain multi-wavelength second-harmonic generations [9]. We report in this paper the successful implementation of the SA algorithm to the design of multi-wavelength Šolc-type filters based on APLN crystals. We also demonstrate, to the best of our knowledge, the first electro-optically active narrowband multi-wavelength APLN filters for use in the telecom C band (~1530-1570nm). In the remaining part of this paper, we abbreviate the name of this multi-wavelength filter as "EO APLN filter".

## 2. Device design and simulation

When modeling the EO APLN filter, we assume the filter consists of a sequence of $N$ crystal-domain blocks, each with a thickness of $\Delta x$ and a domain polarity of either +1 or −1 denoting the +z or −z crystal orientation of the block, respectively. Consider the *ordinary* and *extraordinary* polarization modes, propagating along the APLN crystallographic $x$ axis with the wave numbers $\beta_o$ and $\beta_e$, respectively. When an external electric field $E_y$ is applied along the APLN crystallographic $y$ axis, the perturbed part of the dielectric tensor of the crystal becomes aperiodically modulated along the $x$ direction due to the sign reversal of the relevant Pockels coefficient $r_{51}$ upon the reversal of the crystal domain in $z$. In the limit of weak perturbation, the power exchange between the two polarization modes in such a dielectric-modulated structure can be described by a pair of co-directional coupled-mode equations [10], given by

$$\begin{aligned} \frac{d}{dx}A_o(x) &= -i\kappa(x)A_e(x)e^{i\Delta\beta x}, \\ \frac{d}{dx}A_e(x) &= -i\kappa^*(x)A_o(x)e^{-i\Delta\beta x}, \end{aligned} \tag{1}$$

where $i$ is the imaginary unit $\sqrt{-1}$, $A_o(x)$ and $A_e(x)$ are the field amplitude envelopes of the ordinary-wave and extraordinary-wave modes, respectively, $\Delta\beta = \beta_o - \beta_e$ is the wave-vector mismatch between the two modes, and $\kappa(x)$ is the coupling coefficient defined by

#81954 - $15.00 USD Received 9 Apr 2007; revised 11 Jul 2007; accepted 17 Jul 2007; published 20 Jul 2007

$$\kappa(x) = \frac{\pi}{\lambda_0}(n_o n_e)^{3/2} r_{51} E_y s(x). \tag{2}$$

In Eq. (2), $\lambda_0$ is the vacuum wavelength of the electromagnetic waves, $n_o$ and $n_e$ are the refractive indices of the ordinary-wave and extraordinary-wave modes, respectively, and the sign function $s(x) = \pm 1$ denotes the $\pm z$ domain polarity of the APLN crystal block at position $x$. If we let $x_j = j\Delta x$ represent the position of the *j-th* block of the APLN for $j = 0, 1, 2\ldots(N\text{-}1)$, the general solution of Eq. (1) at position $x_{j+1}$ can be expressed as

$$\begin{aligned}
A_o(x_{j+1}) &= e^{i\frac{\Delta\beta}{2}x_{j+1}}\{P_1(x_j)\cos rx_{j+1} + P_2(x_j)\sin rx_{j+1}\},\\
A_e(x_{j+1}) &= e^{-i\frac{\Delta\beta}{2}x_{j+1}}\{P_1(x_j)[-\frac{\Delta\beta}{2\kappa(x_{j+1})}\cos rx_{j+1} - \frac{ir}{\kappa(x_{j+1})}\sin rx_{j+1}]\\
&+ P_2(x_j)[-\frac{\Delta\beta}{2\kappa(x_{j+1})}\sin rx_{j+1} + \frac{ir}{\kappa(x_{j+1})}\cos rx_{j+1}]\},
\end{aligned} \tag{3}$$

where $r^2 = |\kappa|^2 + (\Delta\beta/2)^2$ and the functions $P_1(x_j)$ and $P_2(x_j)$ are given by

$$\begin{aligned}
P_1(x_j) &= \sin rx_j(i\frac{\kappa(x_j)}{r}A_e(x_j)e^{i\frac{\Delta\beta}{2}x_j}) + [i\frac{\Delta\beta}{2r}\sin rx_j + \cos rx_j]A_o(x_j)e^{-i\frac{\Delta\beta}{2}x_j},\\
P_2(x_j) &= \cos rx_j(-i\frac{\kappa(x_j)}{r}A_e(x_j)e^{i\frac{\Delta\beta}{2}x_j}) - [i\frac{\Delta\beta}{2r}\cos rx_j - \sin rx_j]A_o(x_j)e^{-i\frac{\Delta\beta}{2}x_j}.
\end{aligned}$$

Assuming the initial conditions, $A_e(0)=0$ and $A_o(0)=1$, for an incident ordinary wave, the transmittance of the optical power in this EO APLN filter can be defined as

$$T = |A_e(x_N)/A_o(0)|^2. \tag{4}$$

The transmittance evidently depends on $\kappa(x)$ and thus on the binary sequence of $s(x)$ and $E_y$. For a given $E_y$, the maximum achievable transmittance at certain wavelengths can be obtained from Eq. (3) by summing the fields from all domain blocks with $s(x)$ optimized from some iteration process.

To find the optimum domain sequence for obtaining equal and maximum transmittance at certain wavelengths, we developed a computer code to calculate Eq. (4) based on the SA algorithm. The algorithm is similar to that used in Gu *et al.*'s work [11] for optimizing second harmonic generation (SHG) with multiple input wavelengths in an aperiodically QPM material. In our computer code, the objective function, which was previously used in Ref. [11] as a convergence criterion for both maximizing and equalizing the SHG conversion efficiencies of prescribed ***M*** SHG output was modified to be

$$Ob = \{\sum_{\alpha=1}^{M}[|T_0(\lambda_\alpha) - T_{cal}(\lambda_\alpha)|]w(\lambda_\alpha)\} + \beta\{\max[T_{cal}(\lambda_\alpha)] - \min[T_{cal}(\lambda_\alpha)]\}, \tag{5}$$

where $T_0(\lambda_\alpha)$, $T_{cal}(\lambda_\alpha)$, and $w(\lambda_\alpha)$ are the expected transmittance, the calculated transmittance from Eq. (4), and the weighting factor at wavelength $\lambda_\alpha$, respectively, $0<\beta<1$ is an adjustable parameter for equalizing peak transmittances, and the operators max[…] and min[…] select the maximum and minimum values among all the possible values of the variable in the square brackets. By using the computer code, we were able to obtain peak transmittance that is a few times larger than the value previously calculated by using the Jones-calculus technique [12] for the same filter length and the same applied electric field. For example, 2.9-time

#81954 - $15.00 USD Received 9 Apr 2007; revised 11 Jul 2007; accepted 17 Jul 2007; published 20 Jul 2007

enhancement in power transmittance was obtained from our computer code when we designed the same four-wavelength filter in a 5-cm long APLN crystal [12]. We also found from our calculation that an EO APLN filter can achieve nearly 100% transmittance for all the design wavelengths at an optimum driving field.

To perform a proof-of-principle experiment, we designed an EO APLN filter that transmits 8 International Telecommunication Union (ITU) wavelengths, $\lambda_1$= 1541.34, $\lambda_2$= 1543.73, $\lambda_3$= 1546.11, $\lambda_4$= 1548.51, $\lambda_5$= 1550.91, $\lambda_6$= 1553.32, $\lambda_7$= 1555.74, and $\lambda_8$= 1558.17 nm, at 37.5°C with a 300-GHz frequency separation between adjacent channels. In the computer code, we set the parameters $T_0(\lambda_\alpha)$= 1 and $w(\lambda_\alpha)$= 1 for $\alpha$= 1, 2, 3,…,8 to maximize the transmittances at all the 8 designated wavelengths with equal weighting. We chose β= 0.4 in Eq. (5) to ensure equalization of the peak transmittances. Although a short domain thickness $\Delta x$ is preferred for optimizing the device performance, we chose $\Delta x$= 5 μm to meet our current ability in $LiNbO_3$ crystal poling. The total number of the domain blocks was set to be 10000 so that the length of the EO APLN filter was 5-cm. Figure 1(a) shows the calculated transmittance of the 5-cm long APLN filter (green curve) as a function of the applied electric field, from which we determine an optimum driving field of 277 V/mm at the peak transmittance. The green curve in Fig. 1(b) shows the transmittance of the filter as a function of the input wavelength at the optimal driving field, indicating nearly 100% transmittance for all 8 channels in our design. According to the green curve in Fig. 1(b), the noise floor for polarization cross-talk is approximately 25 dB lowered from the peak transmittance. For slowly varying field envelopes in the filter, the output field amplitudes are proportional to the Fourier transform of $s(x)$ evaluated at the spatial frequency $\Delta\beta = \beta_o - \beta_e$, according to Eqs. (1, 2). Therefore the applied field $E_y$ has a negligible effect on the transmission wavelengths of the filter. However, the coupling coefficient $\kappa$ and thus the transmittances are dependent on $E_y$. As shown by the black dashed curve in Fig. 1(b), the transmission spectrum of the filter driven by an intermediate field of 100 V/mm shows the same peak transmission wavelengths but has lower peak transmittances.

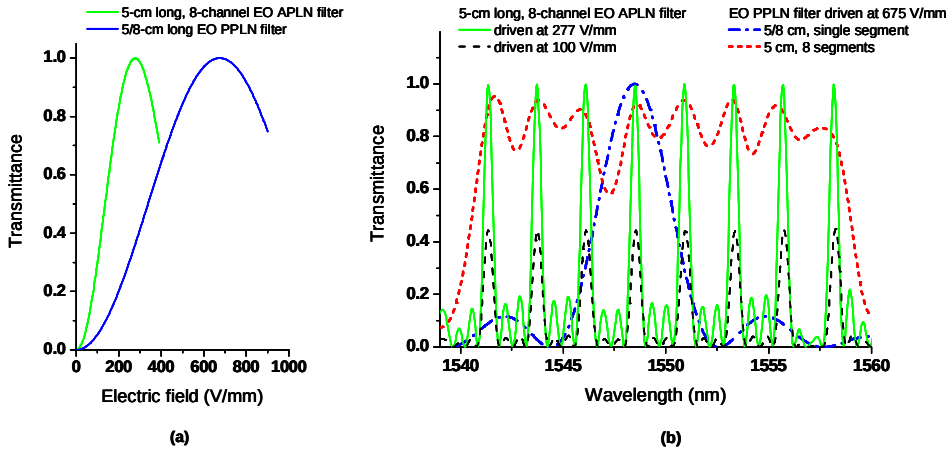


Fig. 1. (a) Calculated transmittance versus applied electric field for the 5-cm long APLN filter (green curve) and a 5/8-cm long PPLN filter (blue curve) phase-matched at 1548.51 nm. The peak-transmission driving field for the PPLN filter is 2.4 times larger than that for the APLN filter. (b) Calculated transmission spectra for the APLN filter driven at the optimal field 277 V/mm (green curve), the APLN filter driven at 100 V/mm (black dashed curve), the single-segment PPLN filter driven at 675 V/mm (blue dash-dotted curve), and the 8-segment cascaded PPLN filter driven at 675 V/mm (red dotted curve). The crosstalk among channels renders the cascaded PPLN filter useless.

#81954 - $15.00 USD Received 9 Apr 2007; revised 11 Jul 2007; accepted 17 Jul 2007; published 20 Jul 2007

In addition, our calculation predicts a signal transmission spectral width of ~0.45 nm for each of the 8 channels at the optimal driving field in the EO APLN filter. We found that the transmission width of a 5-cm long PPLN Šolc-type filter is also about 0.45 nm, despite that a PPLN filter only transmits a single wavelength. If one would cascade 8 equal-length segments of PPLN, each having a length of 5/8 cm and a suitable grating period, to form a 5-cm long Šolc-type filter for transmitting the same 8 ITU wavelengths, this PPLN filter would not only have a much higher driving field but also become impractical due to the crosstalk among the broadened channel peaks. The blue curve in Fig. 1(a) shows the calculated transmittance of a 5/8-cm long single-segment PPLN filter phase-matched at 1548.51 nm as a function of the applied electric field. It is evident from the figure that the driving electric field at peak transmittance for the PPLN filter is increased by 2.4 times from that of the APLN filter. For comparison, we also plot in Fig. 1(b) the transmission spectra of the single-segment PPLN (blue dash-dotted curve) and the 8-segment PPLN (red dotted curve) at the peak-transmission field of 675 V/mm (refer to the blue curve in Fig. 1(a)). It can be seen from the figure that the spectral width of the single-channel PPLN filter is 8.4 times larger than that of the APLN filter. Furthermore, the severe crosstalk and the decreased transmittance render the cascaded PPLN filter useless. The comparison in Fig. 1 indeed unambiguously illustrates the superior performance of an EO APLN filter over a cascaded EO PPLN filter.

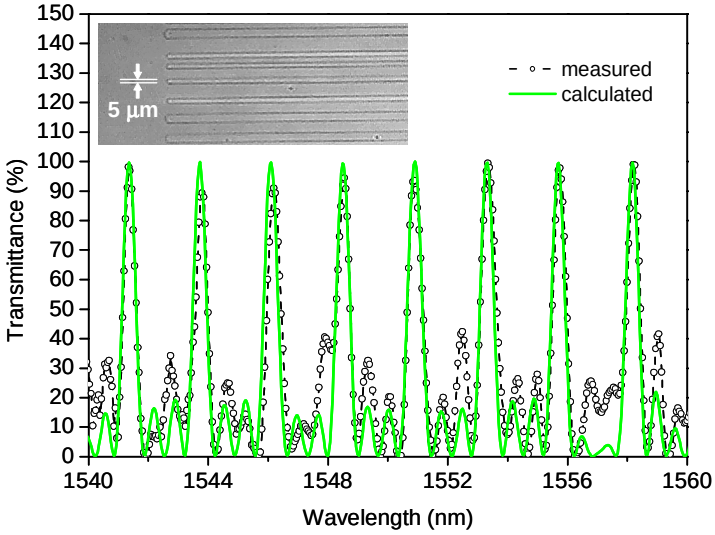


Fig. 2. Calculated (solid line) and measured (open circles) transmission spectra of the 5-cm long EO APLN filter. The two spectral curves agree reasonably well, except that the side lobes in the experimental curve are more apparent. The inset shows a microscopic image of an HF-etched z surface of the fabricated APLN crystal. The label in the inset indicates the width of the unit domain block used in this APLN crystal, i.e., $\Delta x = 5$ μm.

## 3. Experimental demonstration and discussion

We fabricated the APLN crystal by using the conventional electric-field poling technique [13]. The fabricated APLN multi-wavelength filter has a dimension of 5 cm in length, 1 mm in width, and 0.5 mm in thickness. The end faces of the APLN crystal were optically polished but were without any optical coating. The two *y* faces of the APLN crystal were sputtered with NiCr alloy to form side electrodes. The performance of the EO APLN filter was then characterized by using a single-mode, fiber-coupled amplified-spontaneous-emission (ASE) light source in the telecom C band. The output beam of the ASE source was collimated and size-reduced to a radius of ~110 μm in the crystal. The APLN crystal was installed in a

#81954 - $15.00 USD Received 9 Apr 2007; revised 11 Jul 2007; accepted 17 Jul 2007; published 20 Jul 2007

temperature controlled oven with an in-line polarizer at the input end and an analyzer at the output end of the crystal. The transmission axes of the polarizer and the analyzer were aligned along the *y* and *z* axes of the APLN, respectively. Figure 2 shows the calculated (solid line) and measured (open circles) transmission spectra of the 5-cm long EO APLN filter at 37.5°C. The inset shows a microscopic image of an HF-etched *z* surface of the fabricated APLN crystal, which indicates the aperiodicity of the domain structure synthesized from the 5-μm long domain blocks. By inspecting the resulting sequence function $s(x)$ or the fabricated APLN crystal, we found the aperiodic domain structure was composed of 3 different domain thicknesses $\Delta x$= 5 μm, $2\Delta x$= 10 μm, and $3\Delta x$ = 15 μm. Most of the constituent domains have the thickness of 10 μm, which is consistent with the QPM coherence length of 10.62 μm for an EO PPLN device working in the telecom C band [14]. The experimental data in Fig. 2 indicate >90% peak transmittance measured for all the 8 wavelength channels. Although the location and width of each channel are in good agreement with the theoretical predictions, the side lobes in the measured data appear to be more apparent than those in the calculated spectrum. To understand the slight discrepancy between the experimental and calculated results, we first conducted a set of computer simulations similar to that in Ref. [9] to account for the domain-width variations incurred during the electric-field poling process. The simulations indicate that the EO APLN filter is insensitive to this type of fabrication errors, as also concluded in Ref. [9] for APLN wavelength converters. We also investigated the effect of the off-axis incidence of a Gaussian laser beam. The off-axis incident angle changes the spatial harmonic in $s(x)$ and shifts the transmission spectrum. For the laser beam to stay within the 1-mm crystal width over a length of 5 cm, the largest possible incident angle for a 110 μm-waist laser beam is about 15 mrad, as illustrated by the upper-left inset in Fig. 3(a). We calculated this worse-case output spectrum of the EO APLN filter in Fig. 3(a) (green curve). The off-axis incidence of the laser beam indeed causes a slight spectral shift of ~+0.17 nm, but does not give a noticeable change to the peak transmittances. A similar conclusion can be drawn from the estimate of the angular acceptance bandwidth of a QPM nonlinear optical material due to the beam walkoff effect. Following the similar derivation in [15], we obtain the angular acceptance bandwidth for 1% reduction from peak transmittance in an EO PPLN filter, given by

$$\delta\phi_{1\%} = 2\sqrt{\frac{0.6296}{\pi}\frac{n_e}{n_o}\frac{l_c}{L}\cos\phi}\,, \tag{6}$$

where $\phi$ is the laser incident angle relative to the normal to the crystal surface, $L$ is the crystal length, and $l_c$ is the coherence length of the EO QPM process. For $\phi$ = 0, $L$ = 5 cm, and $l_c$ ~ 10.62 μm for telecom C-band wavelengths, the angular acceptance bandwidth $\delta\phi_{1\%}$ in such an EO PPLN filter is approximately 15 mrad. Therefore the divergence and the off-axis incidence of the input laser beam can not be the only source causing the discrepancy.

In our investigation, the discrepancy can be explained by a slight temperature gradient across the longitudinal direction of the 5-cm long APLN crystal in our homemade crystal oven. The red curve in Fig. 3(a) shows the simulation result for the 5-cm long EO APLN filter with a temperature gradient of –0.1°C/cm decreased from the center to both ends of the crystal. With that amount of temperature gradient, the red-curve spectrum in Fig. 3(a) indeed unveils the side lobes and reduced transmittance similar to those in the measured spectrum. To verify this temperature effect, we further fabricated another 1-cm long EO APLN filter designed for filtering four wavelengths in the telecom C band. Figure 3(b) shows a comparison of the calculated and measured output spectra of this short EO APLN filter, indicating excellent agreement between the theory and experiment.

#81954 - $15.00 USD Received 9 Apr 2007; revised 11 Jul 2007; accepted 17 Jul 2007; published 20 Jul 2007

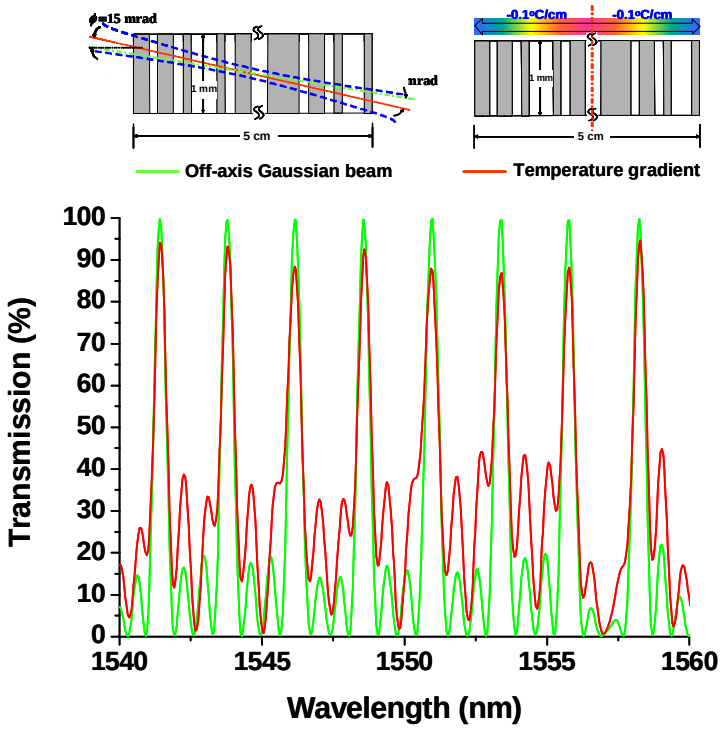


Fig. 3. (a) Green curve: Calculated output spectrum of the 5-cm long EO APLN filter with a 15-mrad laser incident angle and without a temperature gradient in the crystal. The upper left inset illustrates the laser-incidence geometry. Red curve: Calculated output spectrum of the 5-cm long EO APLN filter with a temperature gradient of –0.1°C/cm decreased from the center to both ends of the crystal. The upper-right inset illustrates the temperature gradient in the device. (b) The calculated (red solid curve) and measured (black dotted curve) output spectra of a 1-cm long EO APLN filter, showing a great improvement in the spectral agreement.

#81954 - $15.00 USD Received 9 Apr 2007; revised 11 Jul 2007; accepted 17 Jul 2007; published 20 Jul 2007

Since the refractive indices of the crystal are temperature dependent, it is possible to tune the transmission spectrum of an EO APLN filter by varying the temperature. Figure 4 plots the measured spectral tuning as a function of temperature for the 8 transmitted wavelengths of the 5-cm long EO APLN filter. A tuning rate of ~0.65 nm/$^{o}$C can be derived from the plot.

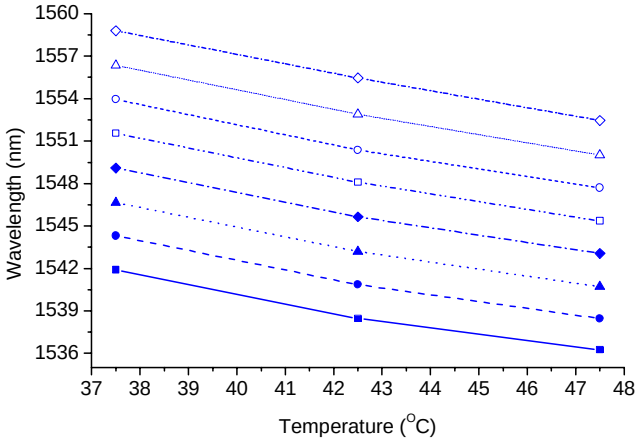


Fig. 4. Measured spectral tuning as a function of temperature for the 8 transmitted wavelengths of the 5-cm long EO APLN filter. The tuning rate is about 0.65 nm/$^{o}$C.

## 4. Conclusion

In conclusion, we have successfully demonstrated active multi-wavelength optical filters by using EO APLN crystals. We derived a coupled-mode theory to model the device behavior and developed a computer code based on the simulated-annealing algorithm to optimize the design of such EO APLN filters. Figure 1 clearly shows the superior performance of an EO APLN multi-wavelength filter over a cascaded EO PPLN filter. In experiment, we simultaneously transmitted 8 ITU-standard wavelengths through a 5-cm long EO APLN filter with a transmittance of >90% and a bandwidth of ~0.45 nm for each wavelength channel. The transmission spectrum of the EO APLN filter can be conveniently tuned by temperature at a rate of ~0.65 nm/$^{o}$C in the telecom C band. We found that the performance of this device is much more sensitive to the temperature gradient than to the domain-width variation in the crystal. Although the EO APLN filter is well demonstrated in the telecom C band, the application of such a filter is apparently not limited to optical communications. To operate at the TTL-level voltage, the EO APLN filter presented in this paper could be implemented in, for example, a Ti-diffused $LiNbO_3$ waveguide [14]. The APLN wavelength filter can also be cascaded with an APLN or a PPLN wavelength converter to perform integrated optical signal filtering and mixing.


## Acknowledgments

This work was supported by the National Science Council (NSC) of Taiwan under NSC Contract Nos. 95-2120-M-001-006 and 95-2221-E-008-161 and partially supported by the Technology Development Program for Academia (TDPA) with Project Code 95-EC-17-A-07-S1-011.


#81954 - $15.00 USD Received 9 Apr 2007; revised 11 Jul 2007; accepted 17 Jul 2007; published 20 Jul 2007